Electronic supplementary information

Smart soft supramolecular hybrid hydrogels modulated by Zn^{2+} / Ag NPs with unique multifunctional properties and applications

Priyanka and Anil Kumar*

Department of Chemistry, Indian Institute of Technology Roorkee, Roorkee - 247667, Uttarakhand, INDIA.
E-mail: anil.kumar@cy.iitr.ac.in; akmshfcy@gmail.com; Tel. +91-1332-285799; Fax. +91-1332-273560

Results

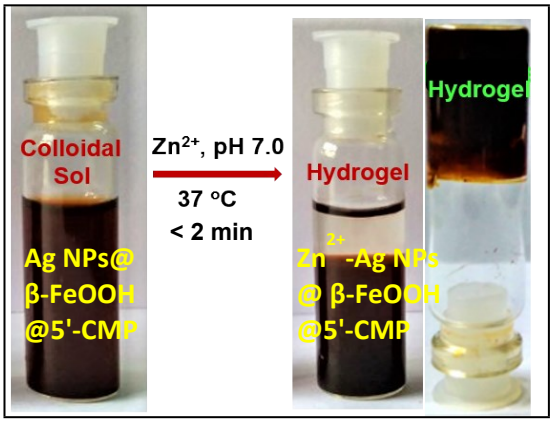

Scheme S1. Digital image exhibiting the synthesis of hydrogel (Zn^{2+}-Ag NPs@β-FeOOH@5'-CMP) *via* colloidal solution formation in self-assembly.

Zeta potential

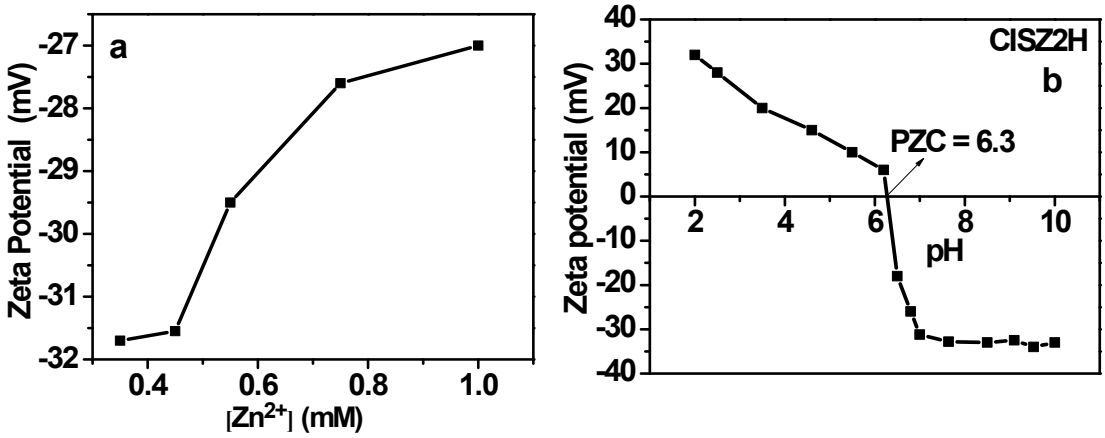

Fig. S1. (a) Zeta potential as a function of $[Zn^{2+}]$, (b) Variation of zeta potential of CISZ2H with pH.

Viscoelastic behaviour

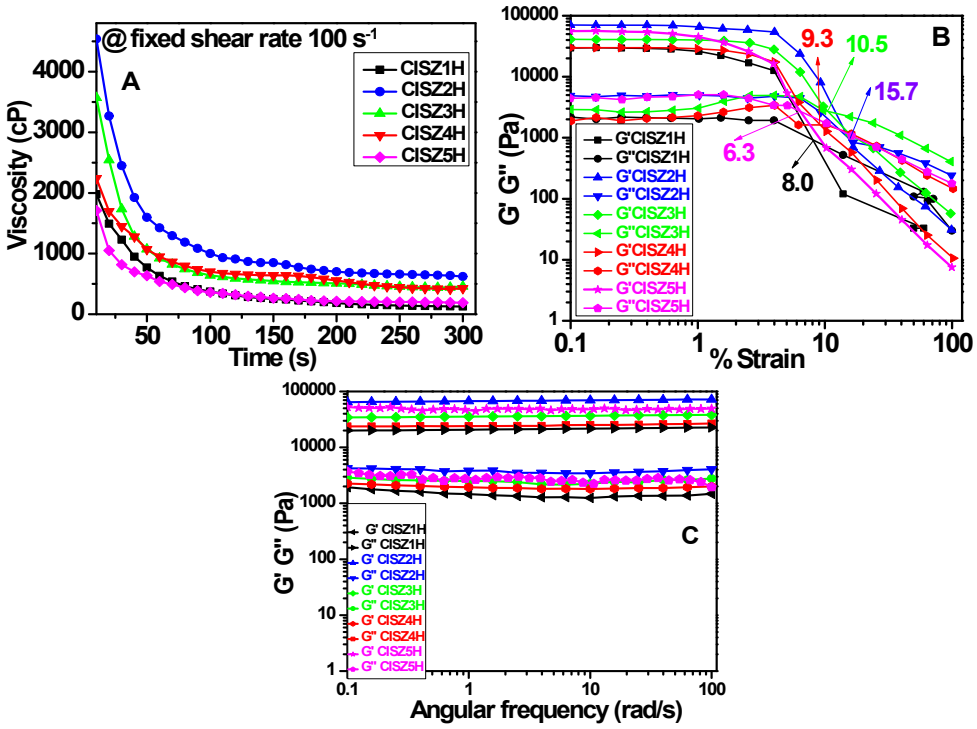

Fig. S2. Rheological properties of hydrogels having different amounts of [Zn^{2+}] ions: (A) Viscosity *vs.* time at fixed 100 s^{-1} shear rate, (B) G'G" *vs.* % strain, (C) G'G" *vs.* angular frequency at fixed strain of 0.5%.

XRD

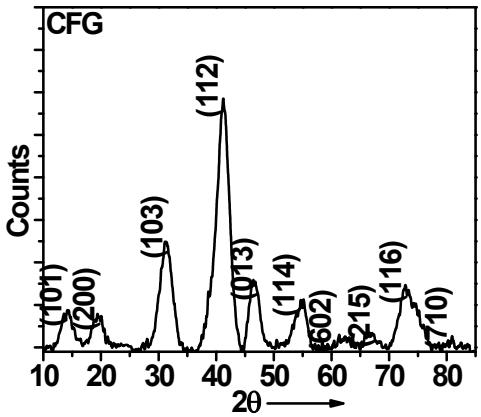

Fig. S3. XRD of base matrix CFG.

TEM and particles size distribution curves

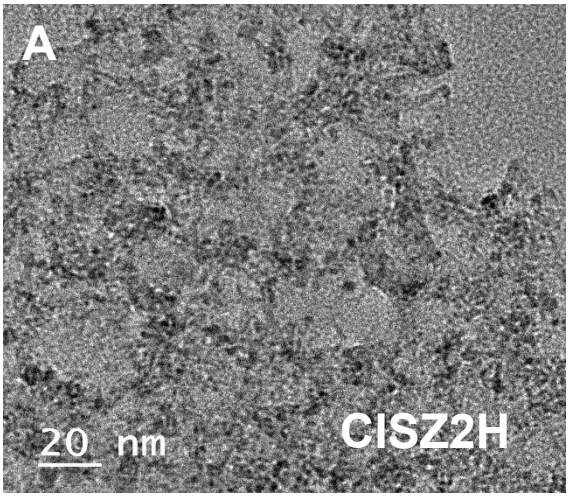

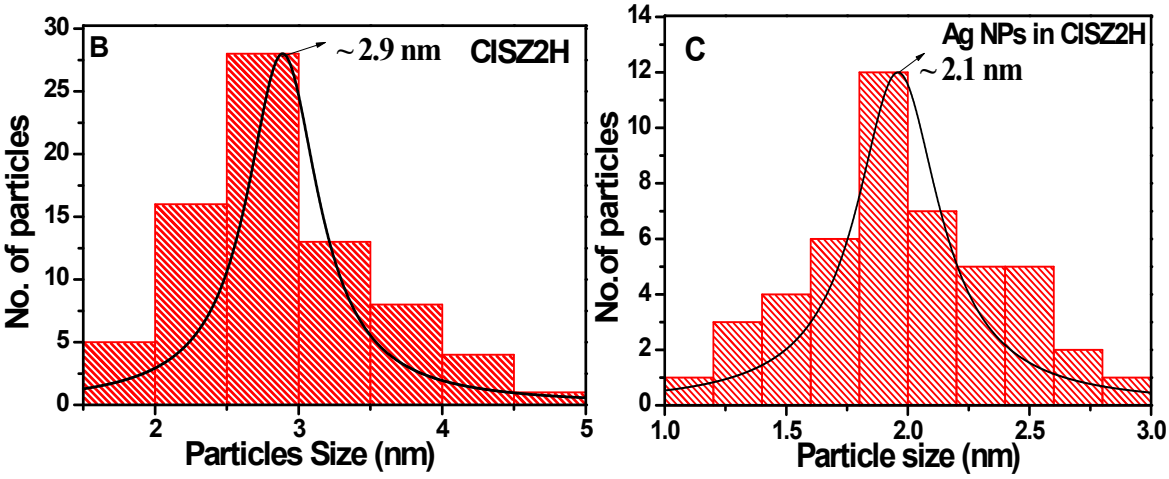

Fig. S4. (A) TEM micrograph of CISZ2H, (B) particle size distribution of β-FeOOH in CISZ2H, (C) particle size distribution of Ag NPs in CISZ2H.

XPS

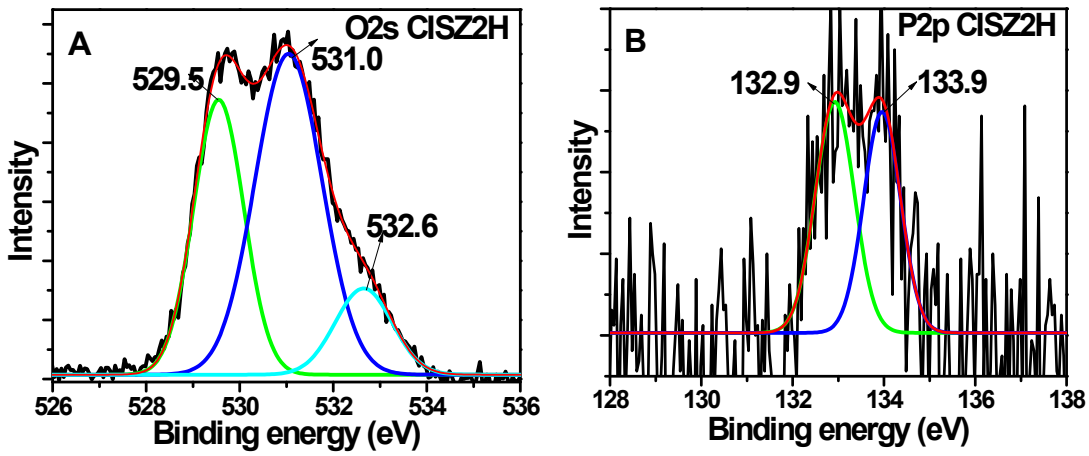

Fig. S5. XPS of elements (A) O, (B) P in CISZ2H.

Pore size distribution

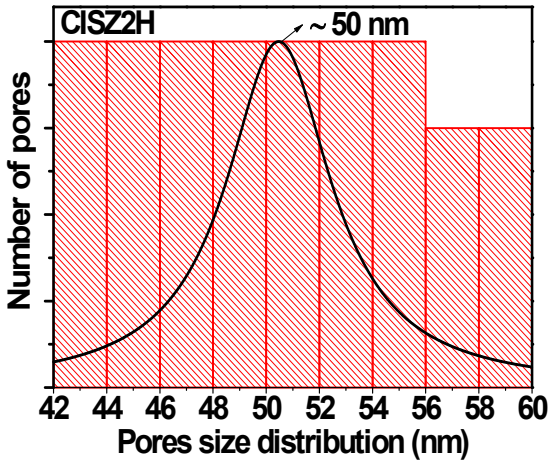

Fig. S6. Pore size distribution in CISZ2H calculated from TEM micrograph shown in Fig. 2, Panel A.

Pore depth and surface roughness in hydrogel

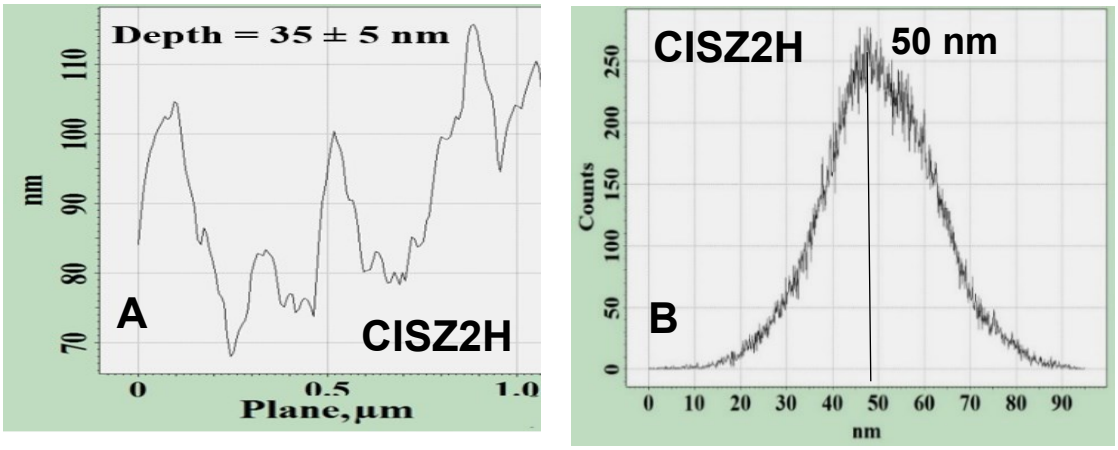

Fig. S7. (A) Pore depth of CISZ2H, (B) Surface roughness of CISZ2H determined from AFM image.

FESEM

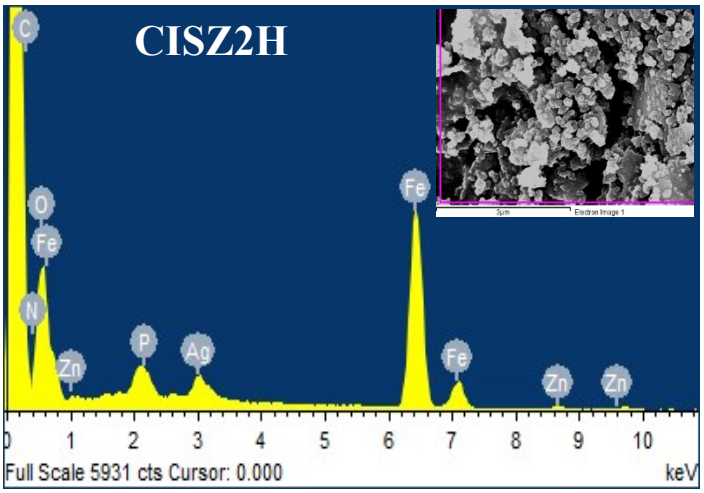

Fig. S8. EDX of CISZ2H determined from FESEM images (inset FESEM image of CISZ2H).

BET measurement

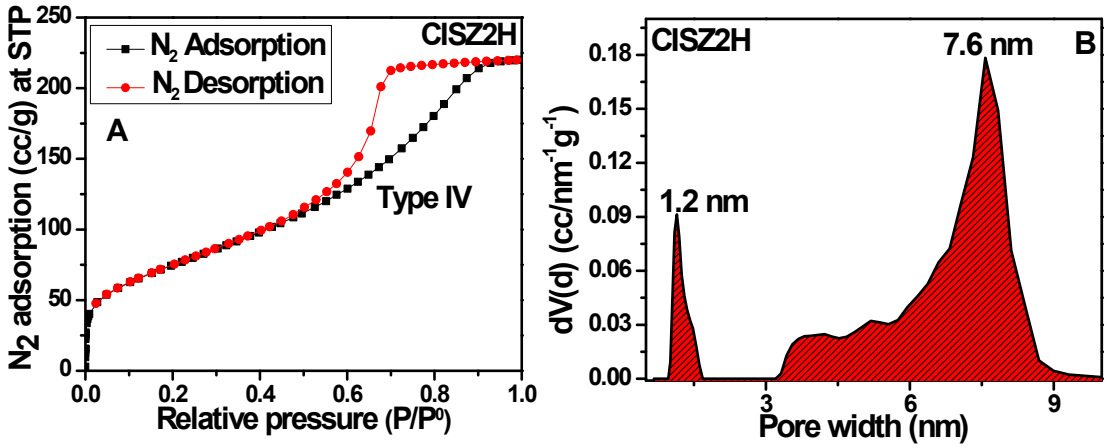

Fig. S9. (A) Adsorption isotherm of FD CISZ2H, (B). Pore width of FD CISZ2H calculated by DFT calculation method.

Magnetic measurements

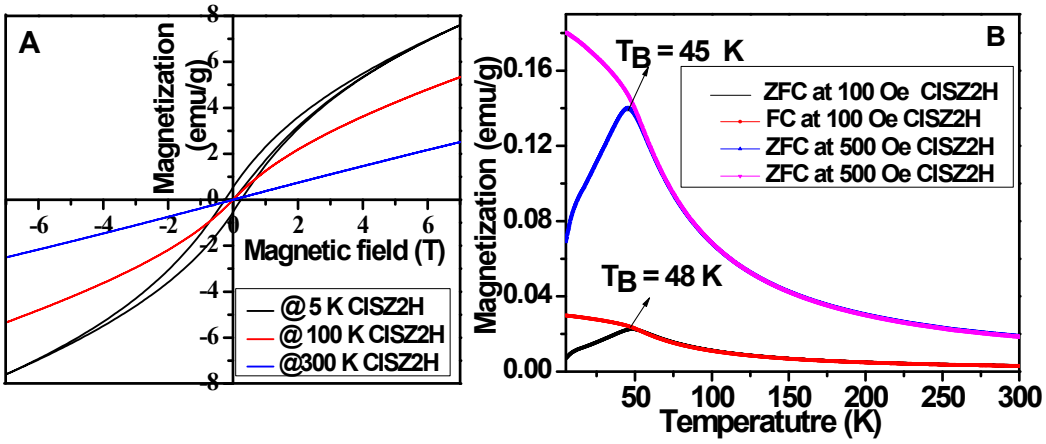

Fig. S10. (A) M-H plots at different temperatures, (B) FC-ZFC plots at 100 O_e and 500 O_e magnetic fields.

M-H plots of FD CISZ2H were recorded in the temperature range of 5 to 300 K. beyond 5 K these plots did not show any remanence (M_r) and coercivity (H_c). At 300 K it exhibited the magnetization value 2.6 emu/g suggesting the superparamagnetic behavior of this hydrogel. The superparamagnetic nature became more apparent at 100 K and which show an increase in the magnetization value to 5.3 emu/g. This sample becomes ferromagnetic at 5K. The

superparamagnetic nature below blocking temperature was also verified by recording FC-ZFC curves.

Raman spectra

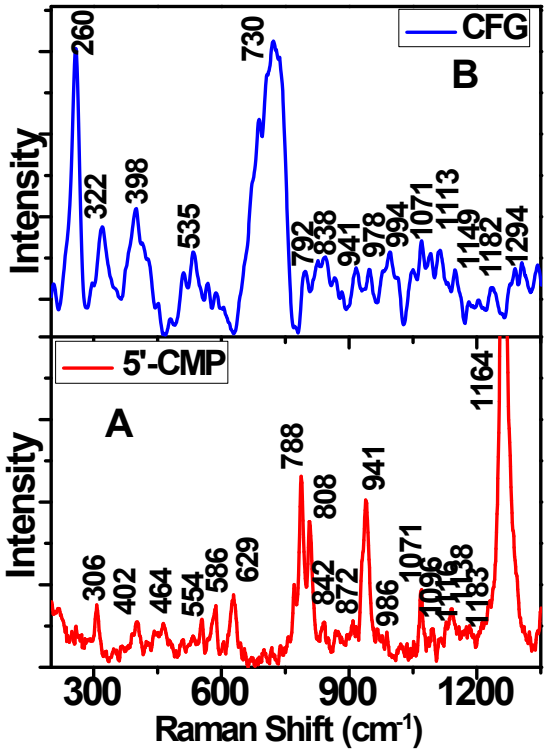

Fig. S11. Raman spectra of: (A) pure 5'-CMP, (B) base matrix CFG.

%Swelling of freeze dried (FD) hydrogel

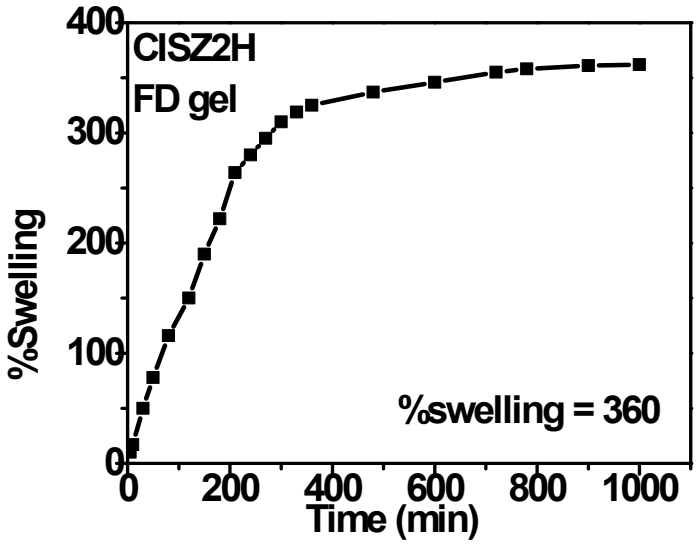

Fig. S12. %Swelling of FD gel.

Cytotoxicity study

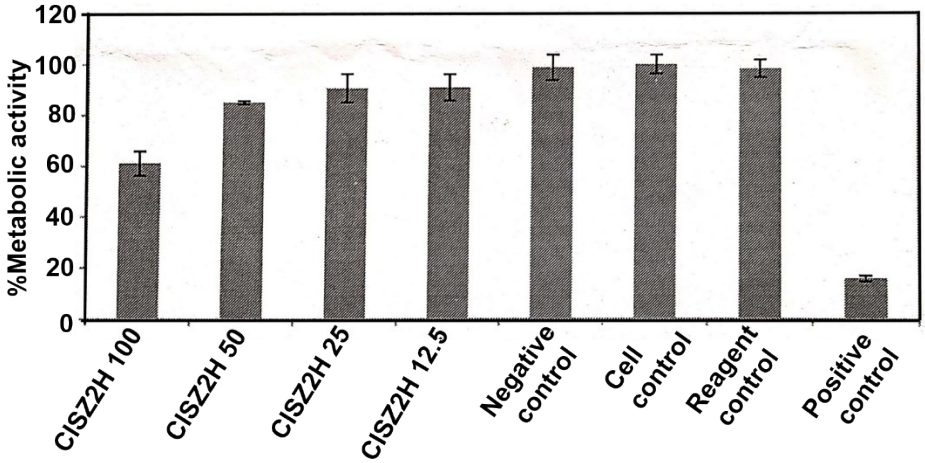

Fig. S13. Cytotoxicity of CISZ2H for its different percentage against L-929 cell line.

% Release of MB

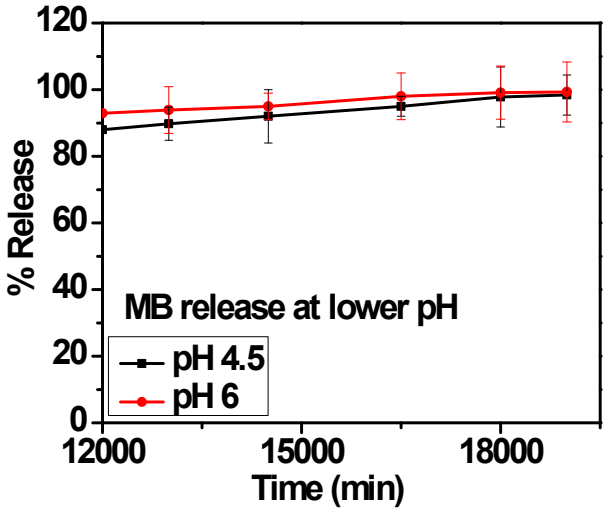

Fig. S14. Complete %release for MB at lower pHs 4.5 and 6.0.

SERS measurements

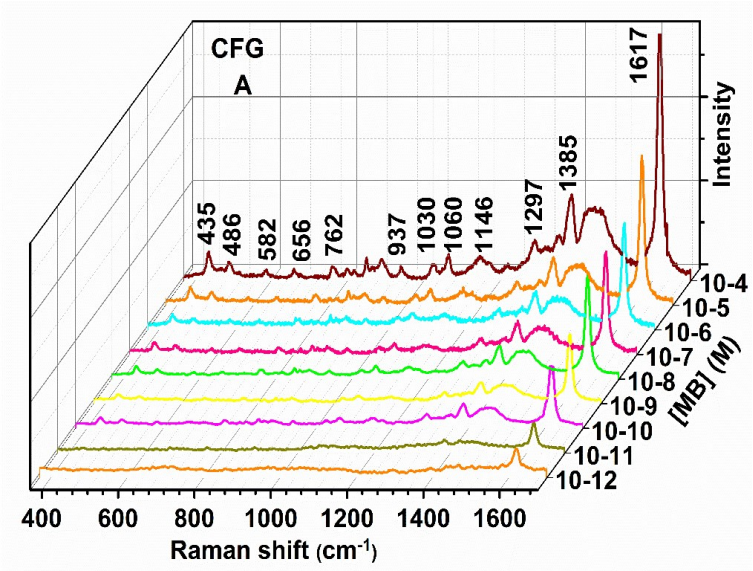

Fig. S15. SERS measurements of CFG for different [MB].

Lower limit of detection (LOD)

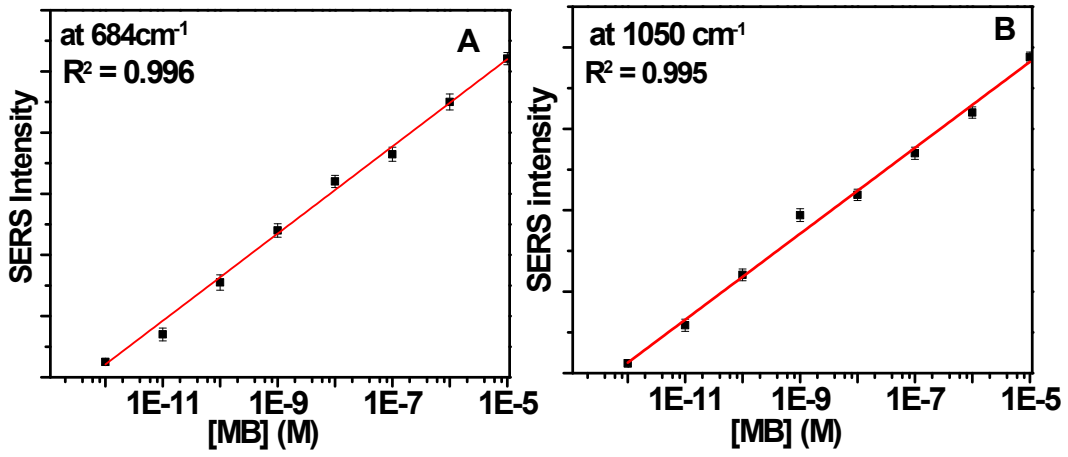

Fig. S16. LOD for MB: (A) SERS intensity *vs* [MB] at 684 cm^{-1} (B) SERS intensity *vs* [MB] at 1050 cm^{-1}.

Dynamic light scattering (DLS) measurement

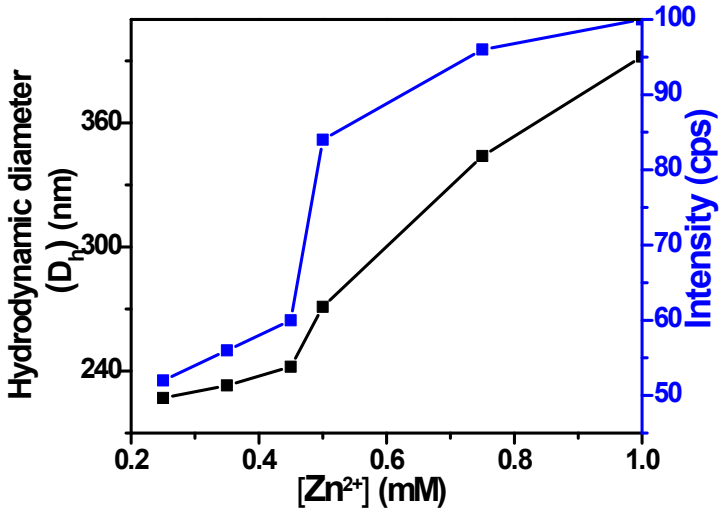

Fig. S17. Plots of scattered light intensity and hydrodynamic diameter as a function of $[Zn^{2+}]$ ions.

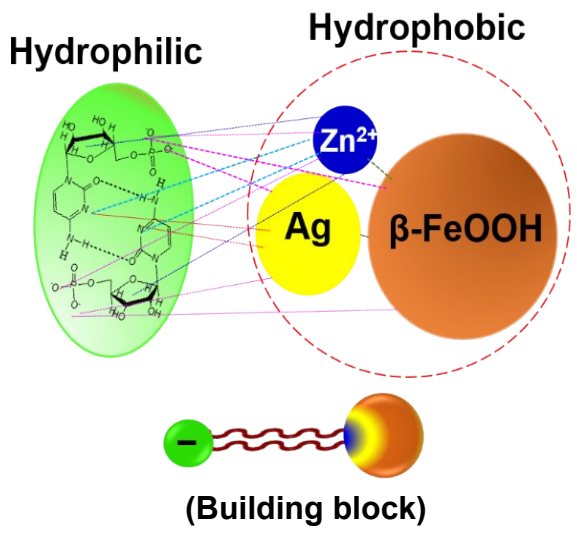

Scheme S2. 5'-CMP mediated ternary nanohybrids forming building block.

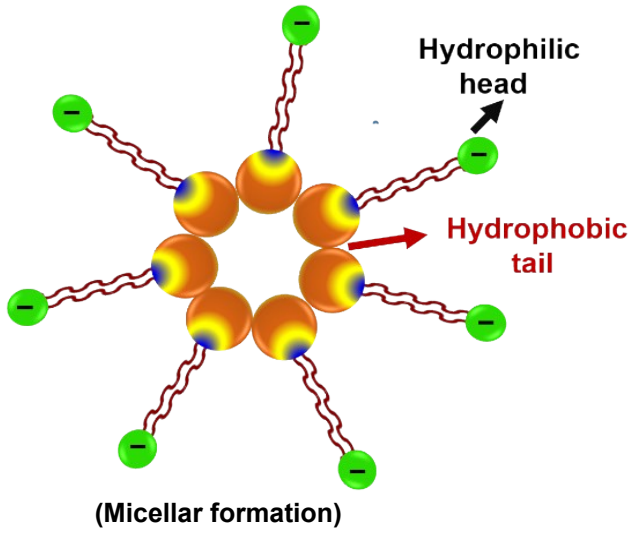

Scheme S3. Micelle formation *via* aggregation of building blocks.

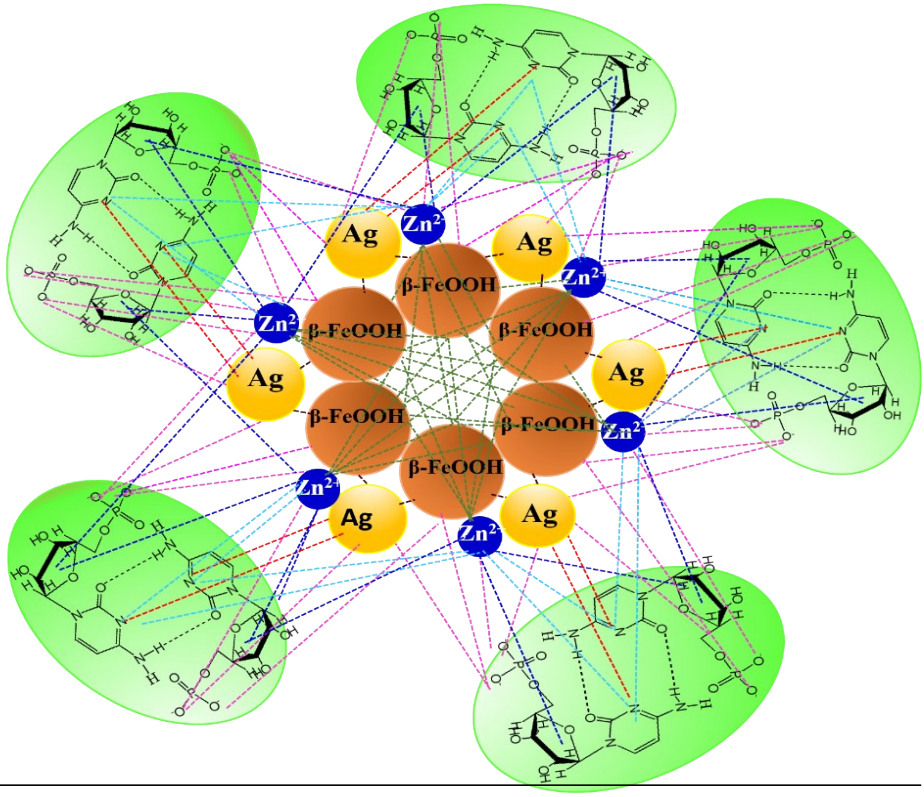

Scheme S4. Zn^{2+}/Ag NPs inducing puckering of ribose sugar in 5'-CMP enhancing non-covalent interactions among different building blocks.

Table S1. Rheological data of hydrogels samples containing different [Zn^{2+}] ions

Sample	Viscosity (cP)	Storage modulus (Pa)	Loss modulus (Pa)	Yield strain (%)
CISZ1H	2014	30216	2190	8.0
CISZ2H	4500	71206	4944	15.7
CISZ3H	3550	40788	2956	10.5
CISZ4H	2264	31539	2010	9.3
CISZ5H	1728	57471	4538	6.3

Table S2. Binding energies (eV) of different elements present in CISZ2H in XPS measurement

Elements	Bulk energy (eV)	CISZ2H energy (eV)
Fe	710.7, 717.7, 724.3	710.1,711.0, 717.7, 724.0, 725.5
Ag	367.9, 373.9	367.7, 373.7
Zn	1021.45, 1044.55	1021.6, 1044.7
N	397.9	398.5, 399.9, 400.8
O	531.6	529.5, 531.0, 532.6
C	284.6	284.6, 286.0, 286.9, 288.3
P	132.9	132.9, 133.9

Table S3. Elemental analysis recorded by FESEM for CISZ2H

Element	Weight%	Atomic%
C K	37.19	48.88
N K	11.45	12.91
O K	33.87	33.42
P K	0.28	0.14
Fe K	15.22	4.30
Zn K	0.62	0.15
Ag L	1.37	0.20
Totals	100.00	

Table S4. BET measurement for FD CISZ2H

Sample	Surface area (m^2/g)	pore width (nm)	Pore volume (cc/g)
CISZ2H	300 ± 6	1.2 nm (micro) and 7.6 nm (meso)	0.328

Table S5. Magnetic data of CISZ2H

Sample	Magnetization (emu/ g) @5 K	Magnetization (emu/ g) @ 100 K	Magnetization (emu/ g) @ 300 K	Coercivity (H_c) (T) @ 5K	Remanence (M_r) (emu/ g) @ 5 K
CISZ2H	7.5	5.3	2.6	0.24	0.53

Table S6. Raman data for different samples

Assignment of peaks	Raman peaks for different sample(s) (cm^{-1})				
	Cytidine literature observed peaks	5′-CMP observed peaks	β-FeOOH observed peaks	CFG observed peaks	CISZ2H observed peaks
Fe-O vib. of octahedral Fe site	-	-	322	322	317 (red shift)
Fe-O vib. of octahedral Fe site	-	-	388	398	388(red shift)
	-	-	539	535	527(red shift)
	-	-	720	730	716(red shift)
Zn^{2+}	-	-	-	-	156, 247
RS	408	402	-	-	diminish
C+RS	456	464	-	-	diminish
δ(C2-N3=C4) and δ(N1-C2-N3)	560	554	-	-	diminish
C2=O2 bending	600	586	-	-	591(blue shift)
δ(N1-C1'-O)	626	629	-	-	diminish
(C5-C4-N4)	714	700	-	-	716
Ring breathing	792	788	-	792	795(blue shift)
P-O str.	818	808	-	-	diminish
δ(C2'-C1'-O).	844	842	-	838	diminish
RS	870	872	-	-	diminish
δ(O3'-C3'H)	944	941	-	941	945 (blue shift)
Out of phase δ(C4-N4H) / PO_3^{2-} str.	986	986	-	978, 994	974 (red shift)
RS	1074	1071	-	1071	1050 (red shift)

(νC4'O-νC4'C3'-δC3'O3')	1117	1116	-	1113	1125 (blue shift)
δ(C2'C1'H), rNH_2, δ(O1'C1'H)	1138	1138	-	1149	diminish
ν(C1'-N1)	1194	1184	-	1182	1195 (blue shift)
C+RS	1252	1265	-	-	diminish
δ (C2'-C1')	1291	-	-	1294	diminish

* **C** = Cytosine, **RS** = ribose sugar, δ = bending mode, ν = stretching mode, r = rocking mode.

Table S7. IR data for different samples

Functional Group/ assignments of peaks		**IR peaks observed for different sample(s) (cm^{-1})**				
	β-FeOOH literature peaks	**β-FeOOH Observed peaks**	**5'-CMP literature peaks**	**5'-CMP Observed peaks**	**CFG Observed peaks**	**CISZ2H Observed peaks**
Fe-O-Fe str.	420, 471, 644, 696	427,480, 641, 696	-	-	472,707 (br)	472
Fe-OH- -Cl deformation	815, 833	837(s)	-	-	diminish	diminish
Bending vib. of H_2O	1632	1632(s)	-	-	1632	diminish
Base bending mode	-	-	555	546	diminish	diminish
δ(N1-C1'-O4')	-	-	621	601	601	diminish
δ(C2'-Cl'-N1), δ(Nl-Cl'-O4')	-	-	630	630	652(br.)	650
δ (C5-C4-N4)	-	-	715	717	707	710
(br)Ring breathing	-	-	790	786	790(br.)	793
P-O str.	-	-	817	817	diminish	diminish
δ(C2'-Cl'-O4')	-	-	845	-	852	diminish

Ribose sugar In phase δ (C4'C5'H)	-	-	872	872	diminish	diminish
Ribose sugar δ (O3'C3'H)	-	-	943	941	diminish	diminish
$-PO_3^{2-}$sym. Str., $-NH_2$ bending	-	-	985	980	984(br.)	981
δ(N1-C1'H)	-	-	1054	1050	1066 (br)	1069
$-PO_3^{2-}$ deg.	-	-	1080	1077	diminish	diminish
(νC4'O-νC4'C3'-δ C3'O3')	-	-	1117	1117 (br)	1113(s)(br) new band	1121
δ(C2'C1'H), r(NH2), δ(O1'C1'H)	-	-	1154	1147	diminish	diminish
Ribose sugar δ(C2'O2'H)	-	-	1213	1222	1216	1219
C+RS	-	-	1248	1255	diminish	diminish
C+RS	-	-	1294	1298	1286	1290

C = cytosine, **RS=** ribose sugar, δ = bending mode, ν = stretching mode, r = rocking mode,
deg. = degeneracy, br = broad, s = sharp, red = reduce.

Table S8. SERS data for MB on CISZ2H and on CFG hydrogel samples

Raman Peaks of Pure MB (cm^{-1})	**Raman Peaks of MB on base matrix CFG (cm^{-1})**	**Raman Peaks of MB on CISZ2H (cm^{-1})**	**Assignment of Peaks**	**Relative Enhancement Factor calculated due to MB observed on CISZ2H to that on CFG for its varied concentrations ranging from 10^{-5} - 10^{-12} M**
435	435	462	Skelton deformation of C-N-C	4.9 ± 0.8
488	486	516	Skelton deformation of C-N-C	5.5 ± 0.5
580	582	610	Skelton deformation of C-S-C	2.2 ± 0.4
660	656	684	Out of plane	6.4 ± 0.1

			bending of C-H	
760	762	784	In plane bending of C-H	6.3 ± 0.1
940	937	964	In plane bending of C-H	4.1 ± 0.3
1030	1030	1050	In plane bending of C-H	11 ± 0.5
1060	1060	1082	C-N stretching	4.3 ± 0.4
1143	1146	1168	In plane C-H bending	5.2 ± 0.3
1291	1297	-	C-C ring stretching	-
1383	1385	1406	Symmetrical C-N stretching	2.4 ± 0.4
1455	1430	-	Asymmetrical C-N stretching	-
1614	1617	1640	C-C ring stretching	3.5 ± 0.1

The relative SERS enhancement factor was calculated by using the following formula:

$$Relative\ SERS\ Enhancement\ Factor = \frac{I_{SERS(CISZ2H)}\ N_{CFG}}{I_{Raman(CFG)}\ \ N_{CISZ2H}}$$

Where $I_{SERS\ (CISZ2H)}$ and $I_{Raman\ (CFG)}$ represent the intensities of peaks recorded on CISZ2H (in the presence of Zn^{2+} ions and Ag NPs) and on CFG (in the absence of Zn^{2+} ions and Ag NPs), respectively. N_{CFG} and N_{CISZ2H} denote the initial concentration(s) of MB on CFG (in the absence of Zn^{2+} ions and Ag NPs) and CISZ2H (in the presence of Zn^{2+} ions and Ag NPs), respectively.

Table S9. Susceptibility of CISZ2H for different bacterial strains

Sample	**Bacterial strains**	**Pathogen/ nonpathogenic**	**Gram (+/-)**	**MIC (µg/ml)**
CISZ2H	*Salmonella typhi*	pathogenic	(-)	25
	Staphylococcus aureus	pathogenic	(+)	50
	Pseudomonas aeruginosa	pathogenic(MDR)	(-)	100
	E. Coli	pathogenic	(-)	250